FORMATION OF CERAMIC PARTICLES IN INTERMETALLIC Ti-46Al-2W-0.5Si ALLOY DURING DIRECTIONAL SOLIDIFICATION

JURAJ LAPIN[1]*, ĽUBOŠ ONDRÚŠ[1]

Formation of ceramic particles in intermetallic Ti-46Al-2W-0.5Si (at.%) alloy directionally solidified in alumina moulds was studied. The ceramic particles formed due to a reaction between the melt and the mould were identified to belong to α-Al_2O_3 phase. The reaction was found to occur preferentially at the mould grain boundaries. The diffusion controlled attack of grain boundaries resulted in a release of grains from the mould. Moving solid-liquid interface assured homogenous redistribution of the particles from the reaction zone into the whole volume of directionally solidified ingots. Increasing reaction temperature and time increased volume fraction and size of the particles. The volume fraction of particles was found to follow $V_c \propto t_r^m$ law with the time exponent of $m = 0.62$, and the activation energy for particle formation was determined to be $Q = 375$ kJ·mol^{-1}.

K e y w o r d s: intermetallics, titanium aluminides, crystal growth, kinetics, composites

VZNIK KERAMICKÝCH ČASTÍC V INTERMETALICKEJ ZLIATINE Ti-46Al-2W-0,5Si V PRIEBEHU USMERNENEJ KRYŠTALIZÁCIE

Študovali sme vznik keramických častíc v intermetalickej zliatine Ti-46Al-2W-0,5Si (at.%), ktorú sme usmernene kryštalizovali v keramických formách z Al_2O_3. Zistili sme, že keramické častice, ktoré sa vytvárali z dôvodu reakcie medzi taveninou a formou, patria fáze α-Al_2O_3. K reakcii medzi taveninou a formou dochádzalo prednostne na hraniciach zŕn formy. Difúziou kontrolované narušenie hraníc zŕn zapríčinilo uvoľnenie zŕn z formy do taveniny. Pohybujúce sa kryštalizačné rozhranie zabezpečilo homogénnu redistribúciu častíc z reakčnej zóny do celého objemu usmernene kryštalizovaných ingotov. Objemový podiel keramických častíc sa zvyšoval so zvyšujúcou sa teplotou a časom reakcie. Zistili sme, že objemový podiel častíc je možné vyjadriť vzťahom $V_c \propto t_r^m$ s časovým exponentom $m = 0{,}62$ a vypočítali sme aktivačnú energiu vzniku častíc $Q = 375$ kJ·mol^{-1}.

[1] Institute of Materials and Machine Mechanics, Slovak Academy of Sciences, Račianska 75, 831 02 Bratislava 3, Slovak Republic

* corresponding author, e-mail: ummslapi@savba.sk

1. Introduction

Ordered TiAl based alloys have been extensively studied as potential high-temperature materials for low pressure stage of gas turbine engines or for turbocharger of diesel engines due to low density, high melting point, good oxidation resistance, and high specific strength. Particularly, alloys based on lamellar microstructure consisting of TiAl (γ-phase) and small volume fraction of Ti_3Al (α_2-phase) are the most promising for structural applications, and an extensive progress has been made in their development [1]. In these alloys the mechanical properties, such as room temperature ductility, high temperature strength, creep and fatigue resistance are very sensitive functions of the microstructure [2–4]. Large effort has been devoted to development of processing techniques aimed at controlling their microstructure. A good combination of room temperature strength, ductility and toughness can be achieved when the lamellar orientation is aligned parallel to the tensile direction. For this reason, directional solidification was developed to produce columnar grain material with the lamellar orientation parallel to the growth direction through appropriate seeding [5–9]. Successful application of directional solidification to production of complex shaped castings necessitates expanding these fundamental studies on cylindrical specimens into the growth of TiAl based alloys in ceramic moulds. Titanium is known as an element reacting with all commercially known ceramic mould materials and is frequently used as a very effective addition element to brazes of ceramics [10]. Therefore, investigations of directional solidification of new titanium intermetallic alloys in ceramic moulds are of great interest.

The aim of this paper is twofold: (1) to study the effect of the reaction time and temperature on formation of ceramic particles in intermetallic Ti-46Al-2W-0.5Si (at.%) alloy during directional solidification in alumina moulds and (2) to evaluate feasibility of directional solidification technique for fabrication of intermetallic matrix composites reinforced with ceramic particles.

2. Experimental procedure

The intermetallic alloy with the initial chemical composition given in Table 1 was supplied in a form of cast cylindrical ingots with a diameter of 21 mm and length of 210 mm. The alloy was developed and provided by Alstom Power (Switzerland). These ingots were cut to smaller pieces, machined to a diameter of 10 mm and length of 100 mm and placed into commercial Al_2O_3 moulds Luxal

Table 1. Initial chemical composition [at.%]

Ti	Al	W	Si	C	Fe	Cu	O	N	H
Bal.	46.23	1.99	0.48	0.017	0.015	<0.001	0.09	0.04	0.08

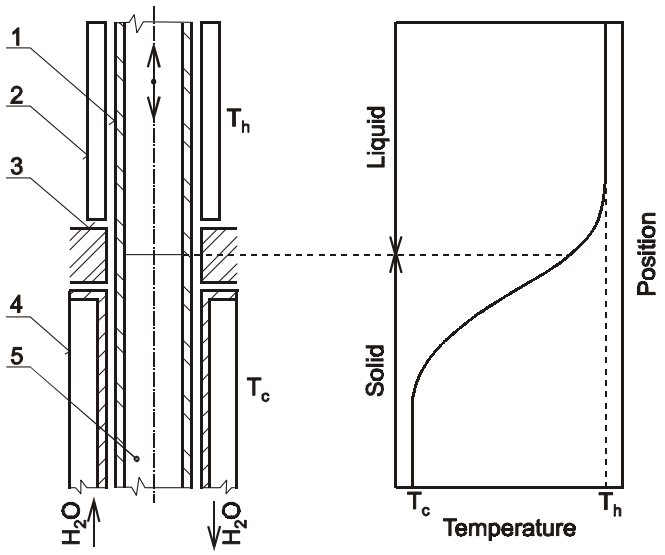

Fig. 1. Schema of directional solidification apparatus: 1 – Al_2O_3 mould; 2 – heating element; 3 – ceramic baffle; 4 – water-cooled crystalliser; 5 – DS ingot; T_h and T_c – temperature of the hot and cold zone, respectively.

203 (mean grain size of 9.3 μm and purity of 99.5 %) of 11/15 mm diameter (inside/outside diameter). Directional solidification was performed under an argon atmosphere in a modified Bridgman-type apparatus [11, 12]. The apparatus is based on withdrawing a mould containing molten alloy from a resistance furnace through a water-cooled copper crystalliser, as sketched in Fig. 1. The parameters that significantly affect reaction between the melt and the ceramic mould are the temperature of the alloy T_h and the withdrawal rate of the mould from the furnace V. For the samples studied in the present work, the alloy was heated to temperatures of 1550, 1600 and 1680 °C. The heating rate to the temperature of T_h was 0.37 °C·s^{-1}, and the melt was stabilised at the temperature for 900 s. Directional solidification was performed at constant withdrawal rates from 2.78×10^{-6} to 1.18×10^{-4} m·s^{-1}. After directional solidification the surface layer of the sample was removed by machining, the sample was turned by 180 degrees and the directional solidification was repeated in a new mould at the same conditions. Such procedure assured constant reaction conditions along directionally solidified (DS) castings. In addition, two types of modified solidification experiments were carried out in the apparatus. First type of experiments consisted of heating of sample to the temperature of T_h, stabilisation at this temperature for various reaction times and switching off the furnace power ($V = 0$ m·s^{-1}). Switching off the furnace power

resulted in a rapid decrease of the sample temperature (cooling rate of about 50 °C $\cdot s^{-1}$). This procedure allowed preserving the distribution of the ceramic particles in the sample, especially in the vicinity of the mould walls. The second type of experiments consisted of heating of sample to the temperature of T_h, stabilisation at this temperature for 900 s, directional solidification at a constant withdrawal rate of V to a length of 55 mm, and quenching. Sample quenching was performed by an abrupt increase of the withdrawal rate to a value of 1.39×10^{-2} m$\cdot$s^{-1}, which assured a fast displacement (time of displacement of 2 s) of the sample from the furnace hot zone to the water-cooled crystalliser. This procedure allowed preserving the morphology of the solid-liquid interface. Assuming the selected withdrawal rates, temperature profile of the furnace, specific types of solidification experiments, and the stabilisation time at the temperature T_h, the reaction time t_r between the mould and the melt was calculated to vary from 2.22×10^3 to 30×10^3 s.

The DS ingots were cut in a direction parallel to the longitudinal ingot axis using a diamond saw. Microstructural analysis was performed by optical microscopy, scanning electron microscopy (SEM), energy dispersive X-ray spectroscopy (EDX), and transmission electron microscopy (TEM). Samples for TEM were mechanically thinned to a thickness of about 100 μm. Thinning was completed by ion milling. Volume fraction and size of ceramic particles were determined by computerised image analysis.

3. Results

Fig. 2 shows the interface between the Al_2O_3 mould and the alloy in a sample that was stabilized at $T_h = 1680$ °C for $t_r = 6.5 \times 10^3$ s and then quenched. The particles are preferentially distributed in a reaction zone formed in the vicinity of the mould wall. The reaction zone contains large number of fine particles and coarser lath-shaped particles protruded from the mould wall into the melt.

The distribution of the particles significantly changed in the DS specimens. As seen in Fig. 3, growing dendrites caused redistribution of particles from the reaction zone into the melt. In spite of the fact that the sample was directionally solidified at $V = 1.39 \times 10^{-5}$ m$\cdot$s^{-1} to a length of 55 mm and then quenched, only several lath-shaped particles are found to be pushed by the moving interface. Hence, the growing dendrites are able to capture the particles continuously and no significant pushing (macrosegregation) occurs during directional solidification. Figs. 4a and 4b show the particles formed at two different withdrawal rates. Both samples contain three types of particles: equiaxed, lath-shaped and clusters of particles. These particles are relatively homogenously distributed in the samples. Fig. 5 graphically summarises the effect of the reaction time and temperature on size of particles. The size is characterised by a mean value of minor axis of the particles calculated from statistical log-normal distribution function. As results

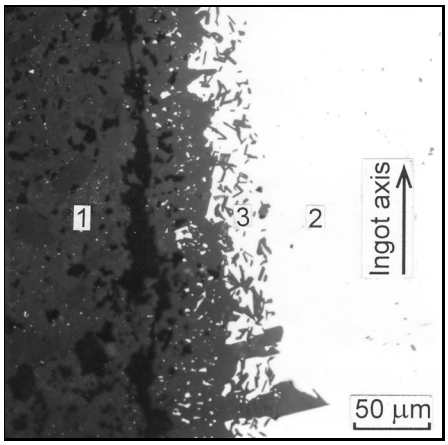

Fig. 2. Optical micrograph showing the distribution of ceramic particles in the reaction zone in a quenched sample prepared at $V = 0\ \mathrm{m\cdot s^{-1}}$, $t_\mathrm{r} = 6.5 \times 10^3$ s and $T_\mathrm{h} = 1680\,^\circ\mathrm{C}$. 1 – mould, 2 – alloy, 3 – reaction zone.

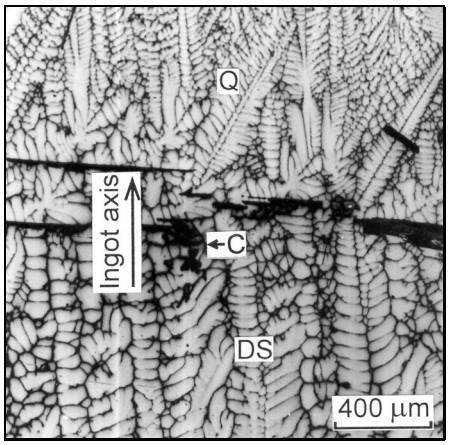

Fig. 3. Backscatter SEM micrograph showing quenched solid-liquid interface, $V = 2.78 \times 10^{-5}\ \mathrm{m\cdot s^{-1}}$, $t_\mathrm{r} = 2.7 \times 10^3$ s and $T_\mathrm{h} = 1680\,^\circ\mathrm{C}$. Q – quenched region, DS – directionally solidified region, C – ceramic particle.

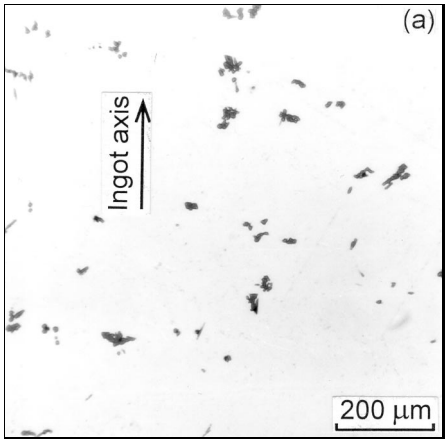

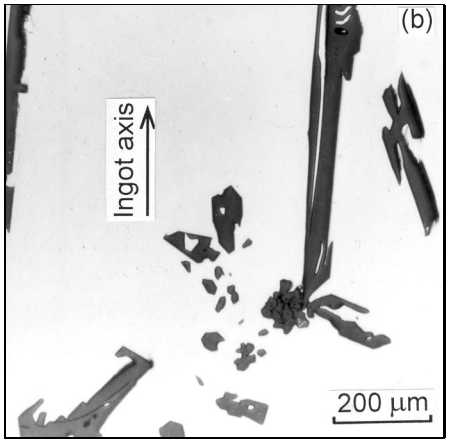

Fig. 4. Optical micrographs showing the particles formed in DS alloy at $T_\mathrm{h} = 1680\,^\circ\mathrm{C}$: (a) $t_\mathrm{r} = 2.22 \times 10^3$ s, $V = 1.18 \times 10^{-4}\ \mathrm{m\cdot s^{-1}}$; (b) $t_\mathrm{r} = 10.1 \times 10^3$ s, $V = 5.56 \times 10^{-6}\ \mathrm{m\cdot s^{-1}}$.

from this figure, the longer reaction time and higher reaction temperature result in a larger particle size.

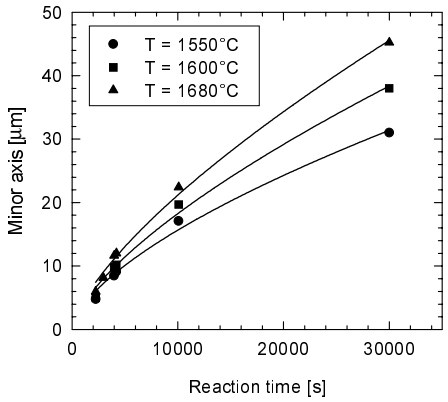

Fig. 5. Dependence of the minor axis of particles on the reaction time. The reaction temperatures are indicated in the figure.

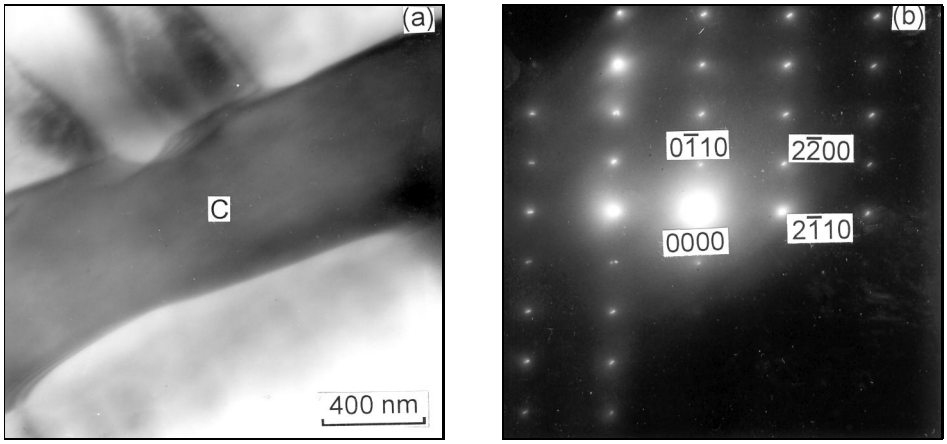

Fig. 6. (a) TEM micrograph showing α-Al_2O_3 particle formed in a central region of DS sample: $t_r = 2.96 \times 10^3$ s, $V = 5.56 \times 10^{-5}$ m·s^{-1}, $T_h = 1680$ °C, C – ceramic particle; (b) corresponding diffraction pattern from $[0001]_\alpha$ zone axis.

Fig. 6a shows TEM micrograph of a particle formed in the central part of DS sample. Corresponding diffraction pattern reveals that the particle belongs to α-Al_2O_3 phase with hexagonal crystal structure, as seen in Fig. 6b. Several diffraction patterns taken from each type of particles (equiaxed, lath-shaped or clusters) as well as EDX analysis (where Al and O content in at.% were measured to be 39.3 ± 0.9 and 60.7 ± 0.9, respectively), confirmed that all particles formed during directional solidification belong to α-Al_2O_3 phase.

Besides the size, the reaction time and temperature affect volume fraction of the particles. Fig. 7 shows the dependence of the volume fraction of particles V_c

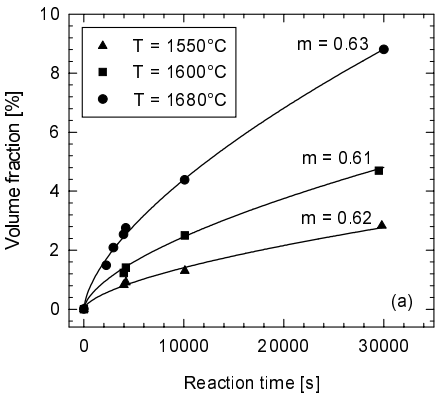

Fig. 7. Dependence of the volume fraction of particles on the reaction time and temperature. The reaction temperatures are indicated in the figure.

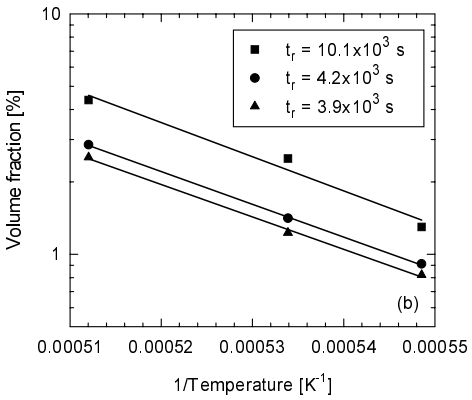

Fig. 8. Arrhenius type of diagram showing the temperature dependence of volume fraction of particles. The reaction time is indicated in the figure.

on the reaction time at three reaction temperatures. The longer reaction time and higher temperature increase volume fraction of Al_2O_3 particles. The volume fractions of particles measured by a computerised image analysis were fitted to a power law

$$V_\mathrm{c} = K t_\mathrm{r}^m, \tag{1}$$

where K is a constant and m is the time exponent. The values of time exponent m determined by regression analysis are reported in Fig. 7. The regression coefficients of these fits, r^2, are better than 0.98. The kinetics of formation of Al_2O_3 particles may be expressed in the form

$$V_\mathrm{c} = K_0 t_\mathrm{r}^m \exp\left(-\frac{Q}{RT}\right), \tag{2}$$

where K_0 is a constant, Q is the activation energy, R is the universal gas constant, and T is the absolute temperature. Fig. 8 shows the temperature dependence of the volume fraction of particles in the form of an Arrhenius plot. The activation energy for particle formation calculated for three different reaction times at three different temperatures is $Q = 375 \pm 18$ kJ·mol^{-1}. The linear regression analysis of experimental data yields an equation in the form

$$V_\mathrm{c} = 1.68 \times 10^8 t_\mathrm{r}^{0.62} \exp\left(-\frac{375000\ \mathrm{J\cdot mol^{-1}}}{RT}\right). \tag{3}$$

The regression coefficient of this fit is $r^2 = 0.97$. The time exponent of $m = 0.62$ indicates that the formation of Al_2O_3 particles is governed by a diffusion [13].

4. Discussion

As shown by Lapin [14], besides Al_2O_3 particles the microstructure of studied alloy contained regular lamellae composed of $\alpha_2(Ti_3Al)$ and $\gamma(TiAl)$ intermetallic phases. In addition, fine Ti_5Si_3 precipitates were identified at interlamellar interfaces, and small amount (less than 1 vol.%) of elongated B2 particles (ordered phase with bcc crystal structure enriched by tungsten and titanium) was found in the interdendritic region. However, formation of fully lamellar α_2/γ microstructure as well as precipitation of Ti_5Si_3 particles occur at lower temperature (about 1300 ℃) by solid state transformations and have no effect on distribution and size of Al_2O_3 particles during solidification.

Microstructural observations revealed that the reaction preferentially occurs at the mould grain boundaries containing impurities and pores (Fig. 2). The diffusion controlled attack of the grain boundaries results in a release of grains from the mould. As shown recently by Duhaj et al. [10], titanium reacts very effectively with Al_2O_3 and forms fine TiO and Ti_2O_3 oxides. Taking into account such mechanisms and assuming ternary Ti-Al-O phase diagrams [15], we can suppose that the reaction might produce phases with the melting point lower than the temperature of the melt. Due to very small density difference between the Al_2O_3 particles ($\rho = 3.9$ g·cm^{-3}) and the studied alloy ($\rho = 3.9$–4 g·cm^{-3}), the particles float in the melt. Moving solid-liquid interface and convection flow in the melt perturb their relatively stable distribution in the reaction zone and redistribute them into the melt.

One mechanism contributing to coarsening of particles in the melt is coalescence of grains released from the mould. Detailed microscopic examination of large lath-shaped particles showed that they are composed of several elongated lath-shaped and equiaxed particles. The second coarsening mechanism might be a direct growth of particles from the melt that could also explain the growth of very long (up to 2 mm) lath-shaped particles. We can only speculate that during the reaction between the melt and mould some amount of free oxygen can be released into the melt contributing to the growth of these particles. This assumption is valid if we consider thermodynamic conditions for formation of complex compounds during the reaction. However, neither TEM analysis nor EDX analysis clearly proved this assumption.

The moving dendritic interface captures the particles by several mechanisms: engulfment by a dendrite tip, entrapment between primary dendrite arms and geometric entrapment [16]. During directional solidification titanium based solid solution with hexagonal crystal structure is the primary solidification phase. The secondary dendrite arms growing at an angle of 60 degrees to the dendrite trunk

represent an effective trap to capture majority of the particles. Several long lath-shaped particles elongated in a direction perpendicular to the ingot axis, such as those shown in Fig. 3, cause instability of the dendritic interface. These particles hinder to a regular diffusion controlled growth of some dendrites by affecting the solute redistribution in the vicinity of dendrite tip radius. Therefore, the neighbouring dendrites, which growth is not affected by such particles, are capable to overgrow the affected dendrites. Developing secondary dendrite arms of the overgrowing dendrites are capable to capture these long lath-shaped particles. Such mechanisms result in microstructure shown in Fig. 9. In an extreme case, during long-reaction time and at low withdrawal rates these large particles serve as nucleation sites for new misoriented grains.

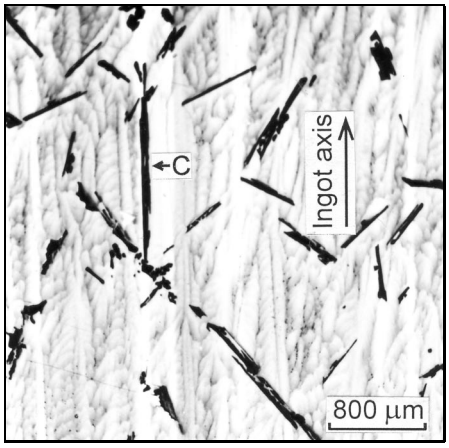

Fig. 9. Backscatter SEM micrograph showing distribution of Al_2O_3 particles in DS ingot: $V = 2.78 \times 10^{-5}$ m·s^{-1}, $t_r = 3.99 \times 10^3$ s, $T_h = 1680\,^{\circ}$C, C – ceramic particle.

5. Conclusions

1. The ceramic particles formed in the intermetallic Ti-46Al-2W-0.5Si (at.%) alloy during directional solidification in alumina moulds were identified to belong to α-Al_2O_3 phase.

2. The reaction between the melt and the mould is found to occur preferentially at the mould grain boundaries. The diffusion controlled attack of grain boundaries results in a release of grains from the alumina moulds. Moving solid-liquid interface causes relatively homogeneous redistribution of the particles from the reaction zone into the whole volume of DS ingots.

3. Increasing reaction temperature and time increase volume fraction and size of the particles. The volume fraction of particles is found to follow $V_c \propto t_r^m$ law with the time exponent of $m = 0.62$ and the activation energy for particle formation is determined to be $Q = 375$ kJ·mol^{-1}.

4. Directional solidification is shown to be a feasible technique for producing intermetallic matrix composites reinforced with homogenously distributed Al_2O_3 particles.

Acknowledgements

The authors would like to thank to Dr. M. Nazmy from Alstom, Baden for providing the material within COST522 – Work Package 1.2 European research programme. The authors gratefully acknowledge the financial support of the Slovak Grant Agency for Science under the contract VEGA 2/1044/21 and the COST 522 project under the contract 51-98-9209-00/1999.

REFERENCES

[1] DIMIDUK, D. M.: Mater. Sci. Eng. A, *A263*, 1999, p. 281.
[2] EVANGELISTA, E.—ZHANG, W. J.—FRANCESCONI, L.—NAZMY, M.: Scripta Metall. Mater., *33*, 1995, p. 467.
[3] NAZMY, M.—STAUBLI, M.—ONOFRIO, G.—LUPINC, V.: Scripta Mater., *45*, 2001, p. 787.
[4] GIL, I.—MUÑOZ-MORRIS, M. A.—MORRIS, D. G.: Intermetallics, *9*, 2001, p. 373.
[5] JOHNSON, D. R.—INUI, H.—YAMAGUCHI, M.: Acta Mater., *44*, 1996, p. 2523.
[6] KIM, S. E.—LEE, Y. T.—OH, M. H.—INUI, H.—YAMAGUCHI, M.: Intermetallics, *8*, 2000, p. 399.
[7] JOHNSON, D. R.—MASUDA, Y.—INUI, H.—YAMAGUCHI, M.: Acta Mater., *45*, 1997, p. 2523.
[8] YAMAGUCHI, M.—JOHNSON, D. R.—LEE, H. N.—INUI, H.: Intermetallics, *8*, 2000, p. 647.
[9] LEE, H. N.—JOHNSON, D. R.—INUI, H.—OH, M. H.—WEE, D. M.— YAMAGUCHI, M.: Acta Mater., *48*, 2000, p. 3221.
[10] DUHAJ, P.—ŠEBO, P.—ŠVEC, P.—JANIČKOVIČ, D.: Mater. Sci. Eng. A., *A271*, 1999, p. 181.
[11] LAPIN, J.: Kovove Mater., *34*, 1996, p. 265.
[12] FLORIAN, M.: Kovove Mater., *38*, 2000, p. 305.
[13] PHILIBERT, J.: Atom Movements – Diffusion and Mass Transport in Solids. Les Editions de Physique, Les Uli 1991.
[14] LAPIN, J.: COST 522 WP 1.2 γ-TiAl—First Progress Report 27 October 2000. ÚMMS SAV, Bratislava 2000, 22 p.
[15] SEIFERT, H. J.—KUSSMAUL, A.—ALDINGER, F.: J. Alloy Compd., *317–318*, 2001, p. 19.
[16] DUTTA, B.—SURAPPA, M. K.: Metall. Mater. Trans. A., *29A*, 1998, p. 1329.

Received: 9.1.2002